

Received 13 July 2025, accepted 30 July 2025, date of publication 10 September 2025, date of current version 30 September 2025.

Digital Object Identifier 10.1109/ACCESS.2025.3608118



RESEARCH ARTICLE

Thermal and Lifetime Analysis of Inverters and Optimisers in Building-Integrated Photovoltaic Applications: A Study on Placement and Environmental Sensitivity

LEANDER VAN CAPPELLEN^{®1,2,3}, ABDELLA ALZADE^{®3,4}, DIRK SAELENS^{3,4}, AND MICHAËL DAENEN^{®1,2,3}

¹Institute for Materials Research (imo-imomec), Hasselt University, 3500 Hasselt, Belgium

Corresponding authors: Leander Van Cappellen (leander.vancappellen@uhasselt.be) and Abdella Alzade (abdella.alzade@kuleuven.be)

This work was supported by the Flanders Innovation and Entrepreneurship and Flux50 through the Project Developing Applied Building Photovoltaics for Performance and Reliability (DAPPER) under Grant HBC.2020.2144.

ABSTRACT This paper presents a comprehensive analysis of how the placement of key power electronic components within building-integrated photovoltaic (BIPV) systems influences their thermal behavior and long-term reliability, focusing on lifetime estimations of the IGBT switches in both inverters and optimisers. A building physics model including the BIPV system was incorporated and integrated within the power electronics device models. This joint model assesses the impact of surrounding conditions on power inverters and optimisers and explores various practical placement scenarios. A sensitivity analysis was conducted under different environmental conditions to evaluate the effects of airflow rates, BIPV ventilation cavity opening dimensions, and radiation-convection ratios on the system's thermal behavior. Results indicate that proper placement strategies with sufficient airflow can significantly enhance cooling, reduce thermal stress, and improve the lifetime of the IGBT. This is particularly evident in the case of the inverter, where the DC IGBT (IGBT in the DC-DC converter stage) located in an isolated ceiling has an increased lifetime consumption of 10.9 % compared to an inverter placed in a utility room. This work provides valuable insights for the design and optimisation of BIPV systems in real-world applications, aiming to improve the operational lifespan of the systems.

INDEX TERMS Building-integrated photovoltaics, lifetime estimation, modeling, power electronics, simulation, thermal management of electronics.

I. INTRODUCTION

The integration of photovoltaic (PV) systems within building envelopes, commonly referred to as Building-Integrated Photovoltaics (BIPV), has emerged as a pivotal technology for enhancing the energy efficiency and sustainability of urban structures. BIPV systems not only provide renewable energy but also contribute to building aesthetics and functionality,

The associate editor coordinating the review of this manuscript and approving it for publication was Chandan Kumar.

making them an attractive solution for green architecture [1]. However, the optimisation of these systems demands precise modeling techniques that integrate thermal, electrical, and architectural factors to ensure performance reliability and longevity of their components [2]. The design of BIPV modules requires thermal management strategies to maximize energy output and extend the operational life of components. Studies underscore the need for integrating thermal and airflow models with electrical models to accurately predict BIPV performance and to compute the module and cell

²imec, imo-imomec, 3590 Diepenbeek, Belgium

³EnergyVille, imo-imomec, 3600 Genk, Belgium

⁴KU Leuven, Heverlee, 3001 Leuven, Belgium



temperature and reflect their effect on the energy yield calculations [3]. This can be accomplished by implementing a coupled thermal-airflow model that captures heat transfer mechanisms (conduction, convection, and radiation) within the module and its surroundings, together with the airflow behavior, offering a comprehensive understanding of thermal dynamics for more accurate performance simulations under diverse environmental conditions [4]. To enhance heat dissipation, BIPV designs often incorporate ventilation cavities. For example, a BIPV module featuring an air cavity facilitates efficient cooling through natural convection. This configuration is critical for maintaining optimal operating temperatures and minimizing thermal stress on components such as inverters [5]. Furthermore, improving ventilation significantly boosts thermal performance by enhancing heat dissipation, thus sustaining efficiency in energy generation [2]. Additionally, the implementation of BIPV requires the presence of a power converter that can perform Maximum Power Point Tracking (MPPT) and convert the voltage to usable levels for consumers. One of the most failureprone components in solar inverters is the power-switching device [6]. These components experience electrical and thermal stress during their lifetime, which can result in abrupt and wear-out packaging failure [7], [8]. Wearout packaging failure is particularly of interest because it can be predicted and anticipated. Wear-out packaging failure is caused by bond wire liftoff, bond wire cracks, and die-attach cracks because of the thermo-mechanical stress resulting from the thermal load cycles the component experiences. Investigating how the BIPV environment influences these load cycles and junction temperature can provide better insight into constructing guidelines for optimal power converter placement. For a more in-depth assessment of BIPV systems, integrating power electronics models with building physics frameworks is crucial. The Modelica simulation environment, with its IDEAS (Integrated District Energy Assessment Simulations) library, is highlighted for its capacity to model complex, multi-domain interactions [9]. This allows functional integration between electrical components and building thermal dynamics, providing a detailed understanding of temperature variations and energy yields in real-time. Modelica's modular approach enables comprehensive modeling, incorporating various elements such as building envelopes, internal heat gains, and renewable energy sources. Sensitivity analyses performed within these integrated models provide insights into how different factors (like radiation-convection ratios and airflow rates) affect the lifetime of Insulated Gate Bipolar Transistors (IGBT) and the overall efficiency of the BIPV system [5]. This study focuses on the complete modeling of the BIPV system, including the power converters, to determine how the BIPV environment influences switching device lifetime. Two types of power converters are considered in this study: DC-DC power optimisers and DC-AC inverters. The study is structured as follows: section II discusses the used electrical, thermal, BIPV, and lifetime models. Next, section III performs a sensitivity analysis for varying boundary conditions, and section IV evaluates the IGBT lifetime for multiple case studies for realistic implementations. Finally, section V ends with a conclusion.

II. METHODOLOGY

This study integrates a comprehensive set of models to assess the thermal and electrical performance of buildingintegrated photovoltaic (BIPV) systems and their associated power electronics, including inverters and power optimisers. This approach aims to capture the interactions between electronic components, BIPV thermal behaviour, and the built environment conditions, enabling a detailed evaluation of system efficiency and longevity. The analysis includes electric and thermal models for both IGBT and BIPV, plus a building physics model, all developed within the Modelica simulation environment, using Modelica base library and the IDEAS library for energy systems modeling. By simulating different component placement scenarios with boundary conditions, the study investigates how environmental and operational factors influence the performance and lifespan of power electronics. The following sections describe the integration process of the implemented models, along with the electrical and thermal modeling approaches for power conversion devices, as well as the BIPV and building physics frameworks.

A. INTEGRATION OF MODELS

The integration of an/a inverter/power optimiser model within the BIPV and building physics models enables a realistic analysis of the electronic components that can be positioned in different locations within the building. The schematics in Fig. 1 and Fig. 2 show the connection mechanism of an inverter thermal model to the building physics model, illustrating how different thermal zones can be incorporated with the power electronics components. The placement zone represents the specific thermal zone of the building where the inverter/power optimiser is located. The zone component includes heat ports that enable thermal interaction between the zone and the power electronics models. These ports account for the heat generated by the electronic components that is transferred to the placement zone to compute the zone temperature and then to the power electronics model, which is used to calculate junction temperatures for lifetime estimation. This mechanism demonstrates a dynamic and interconnected approach where the inverter/power optimiser lifetime model interacts with specific building zones. It uses real-time irradiance and zone temperatures to determine the thermal performance and heat losses of the BIPV-connected inverter system.

B. ELECTRIC MODEL AND CONTROL

This study focuses on two configurations commonly used in PV applications: a full inverter and a power optimiser. The inverter has a two-stage topology: a first DC-DC boost



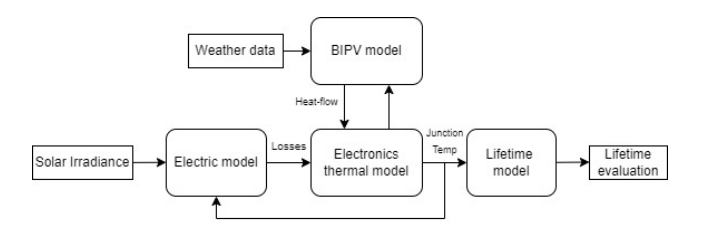


FIGURE 1. Visual summary of all models and how they interact.

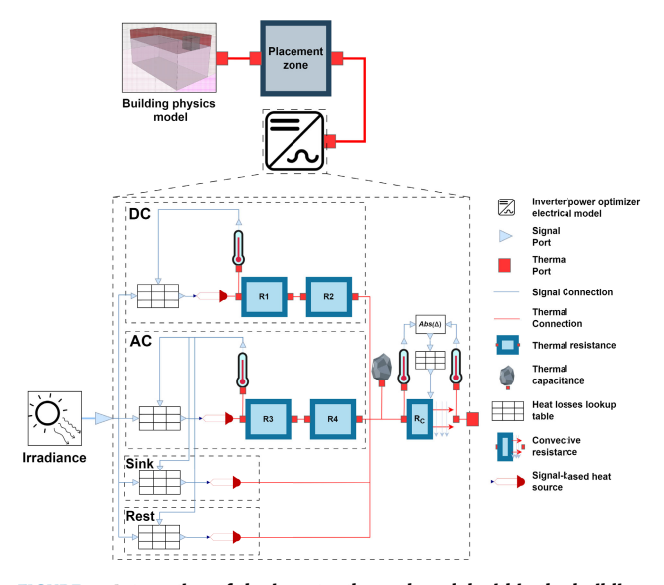


FIGURE 2. Integration of the inverter thermal model within the building physics model.

stage that performs the maximum power point tracking and a second DC-AC step to inject the power into the grid [10]. The full topology is shown in Fig. 3. For the power optimiser case, the same topology is used as the first stage of the inverter [11]. The component configurations are shown in table 1. The switching speed of all switching devices is set to 50 kHz. The voltage over C_{bus} is set to 350 V and 50 V for the inverter and the power optimiser, respectively. For the MPPT control of the DC-DC stage, the Perturb and Observe (P&O) algorithm is used to draw the maximum power from the PV array [12].

A lookup table approach is employed to efficiently calculate all losses of the inverter and optimiser without excessive computational expense. These losses are categorized into two main types. Firstly: losses produced by the passive components. These losses are necessary because they cause passive heating of the inverter and its surrounding environment. However, this study does not focus on analyzing the temperatures of these components. Secondly, the losses are associated with the active components (switches). In this case, the junction temperature plays a critical role, as it is essential for accurately estimating the lifetime of these components. The losses in the switches are dependent on 2 variables: The current and junction temperature. The current is directly related to the solar irradiance. Thus, the lookup tables have 2 dimensions: solar irradiance and

junction temperature. All combinations of switch junction temperature and solar irradiance are applied in the inverter and optimiser, and the simulation is run until a steady state is reached. The losses of all components are collected to create the lookup tables. Note that this lookup table approach eliminates all electric and MPPT transitionary effects. The lookup table assumes that everything is in a steady state and the PV array is in MPP. However, this is not seen as a problem because the simulation resolution in this work is kept at 1 min, which is much longer than the transition effects.

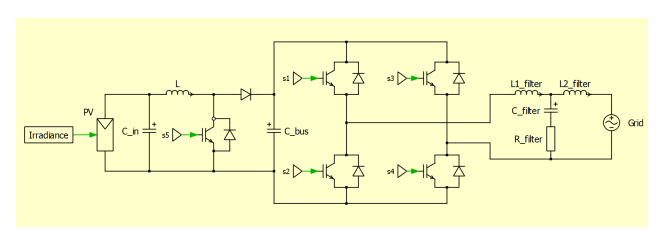


FIGURE 3. Topology of the two-stage inverter.

TABLE 1. Inverter and optimiser component values.

Variable	Value	Unit	
	Inverter		
L	1	mH	
C_in	22	μF	
C_bus	1.5	mF	
L1_filter	2	mH	
L2_filter	3	mH	
C_filter	4.6	μF	
R_filter	10	Ω	
IGBT model	IKZA40N120CS7		
	Optimiser		
L	100	μH	
C_in	10	μF	
C_bus	10	μF	
IGBT model	TPH3R70APL		

C. ELECTRONICS THERMAL MODEL

Since it is preferred for the thermal model to be computationally efficient, accurate, and capable of interfacing with the building physics model, a balance must be struck between simplicity and precision. This ensures that the model remains practical for integration while still providing reliable results for analysis. A widely used method to model electronics thermal behavior is thermal RC networks [11], [13]. The losses, calculated by the electric model, can be divided into three separate groups: DC-switch losses, single AC-switch losses and all remaining switch and component losses as shown in Fig. 4. This approach allows for calculating the junction temperature of the switches. The switch losses are injected into the package and the thermal pad that connects the backplate with the heat sink. The remaining losses are released directly into the sink. The sink releases its heat into the environment with a combination of convection and radiation. As the cooling capacity of a heat sink is dependent



on the heat sink surface temperature, the thermal resistance is modelled as a temperature-dependent variable. The relation between surface temperature and thermal resistance is determined in a finite element simulation by simulating the heat flow from the heat sink to the environment with natural convection for multiple heat sink temperatures [11]. Note that the sink is the only thermal layer that contains a thermal capacitance. Because the simulation takes 1 minute time steps, the smaller capacitance of the switch packaging can be ignored.

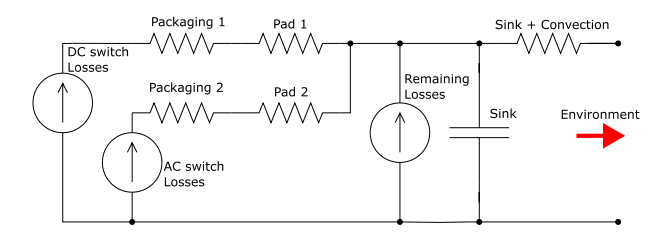


FIGURE 4. Thermal network from DC-switch and AC-switch to ambient.

In the case of the power optimiser, the same approach is used but without the AC switch losses. The values of the thermal resistance of the switch packaging and pad are taken directly from the datasheet. The thermal capacitance of the inverter and the power optimiser sink are determined to be 1283 J/K and 171 J/K, respectively.

MODELICA LANGUAGE AND THE IDEAS LIBRARY

Modelica is a versatile simulation language used for modeling complex systems across different domains [14]. Fundamentally, Modelica is an equation-based modeling language that offers segmentations of a system by creating components and blocks that contain equations for each system or a part of it. This modularity facilitates model reuse, scalability, and the integration of new components or subsystems [15]. The IDEAS Modelica library (Integrated District Energy Assessment Simulation) further enhances Modelica's capabilities by providing numerous detailed models for building and district energy systems. It includes components to simulate energy systems, building dynamics, and fluid networks, which is ideal for capturing the complex interactions in Building-Integrated Photovoltaics (BIPV). This library enables precise modeling of BIPV panels, power electronics, and other components, allowing for comprehensive performance assessments under various operational conditions [9]. Modelica's capacity to model coupled physical systems and domains renders it wellsuited for simulating the physical interactions between the BIPV components and the surrounding built environment. Furthermore, its flexibility facilitates the incorporation of detailed physical models of BIPV panels, power electronic devices, and other BIPV components, enabling comprehensive performance assessments under various operational conditions [16]. Therefore, Modelica was used to model and integrate all the components in this study.

D. BIPV AND BUILDING PHYSICS MODEL

The here implemented BIPV module comprises 24 cells (4×6) arranged in series, encapsulated with 4 mm rear ClearLite glass and front ClearVision glass. The module's backside is connected to a 12 cm air cavity and a 7 cm Rockwool insulation layer. The design includes two ventilation openings (1.01 \times 0.09 m² each) positioned at the top and bottom to facilitate air circulation within the cavity, thereby enhancing heat dissipation. The module is rated to deliver a power output of 120.8 W under standard test conditions (STC). The presented BIPV model is based on the previous work in [5] and [17]. The model comprises two main sub-models: a coupled thermal-airflow model and an electrical model. The coupled thermal-airflow model assesses heat transfer within a BIPV module, considering conduction, convection, and radiation among the module, surroundings, and structure as illustrated in Fig. 5. Additionally, it factors in airflow within the cavity, influenced by buoyancy and wind.

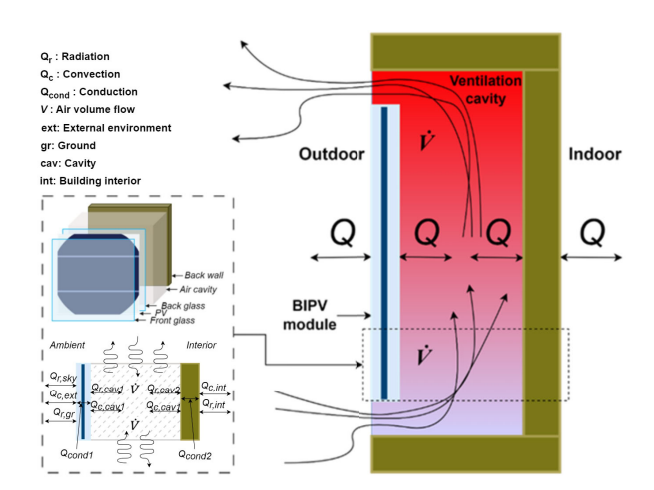


FIGURE 5. Illustration for the heat transfer processes and airflow dynamics in a ventilated BIPV module.

Electrical models of BIPV modules necessitate the plane of array (POA) irradiation from the weather file to compute the electrical output. More advanced models also demand the module temperature to incorporate temperature influences on the power output and the module losses that dissipate in both the outdoor environment and the ventilation cavity, which is accomplished by integrating a thermal model for calculating the module temperature [18]. In this study, the latter method is employed by linking the thermal-airflow model with the electrical model for a more realistic representation of the BIPV behaviour and to include this effect in one of the scenarios in which the inverter/power optimiser is positioned in the ventilation cavity. The variables exchange between the two models is depicted in Fig. 6.

The module has been installed on the south facade of EnergyVille 2 BIPV lab in Genk, Belgium. The data from



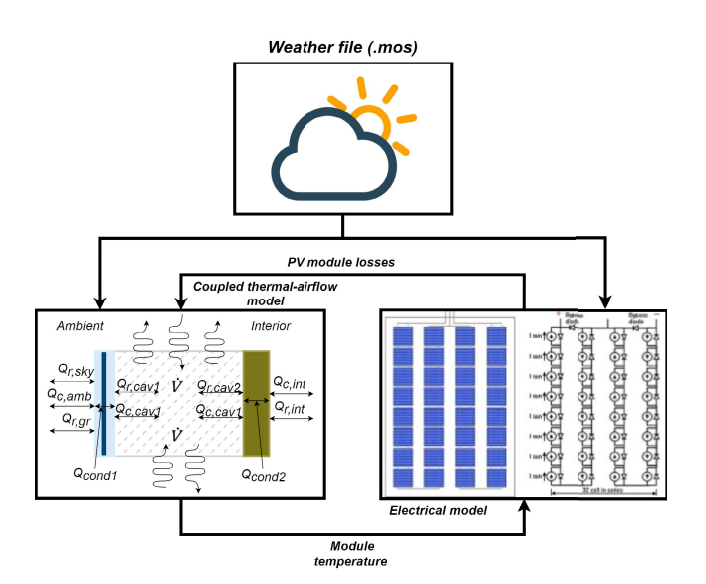


FIGURE 6. Data exchange mechanism between the BIPV coupled thermal-airflow and electrical models.

the building was implemented in the described model for the validation process of the BIPV model. The description and validation of the model are detailed in previous work in [2] and [5].

The projected building physics model in this study is for an office space $(4 \text{ m} \times 3 \text{ m} \times 2.8 \text{ m})$ that features a suspended ceiling hanging 1 m below the concrete construction plate. The office is modelled to be positioned in the center of the south facade of a mid-rise building with dimensions of 30 m in height, 12 m in width and 18 m in depth. These building dimensions are used in determining the convective heat transfer conditions affecting the exterior BIPV façade. Assuming the BIPV to be in the center of the facade simplifies the airflow calculation. Additionally, the bordering zones of the office are considered to have the same thermal condition, hence the interior walls, floor and ceiling are assumed to be adiabatic. The BIPV modules are installed on the facade part of the suspended ceiling. Fig. 7 shows the thermal zone division of the office space.

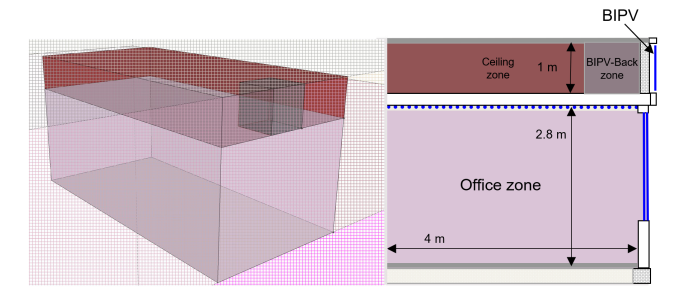


FIGURE 7. Thermal zones division of the office space.

The model includes three components of thermal mixed air zones: one for the office space and two within the suspended ceiling [9]. The division between the office zone and the

ceiling zones is represented by a physical wall component that serves as the suspended ceiling. The ceiling zones are divided into BIPV-Back zone that has a volume of 1 m^3 (1 m× $1 \text{ m} \times 1 \text{ m}$) which is used as a placement scenario and a ceiling zone that represents the remaining volume of the ceiling. The model separates these two zones (BIPV-Back and ceiling zone) by an air-wall, representing thermal division without a physical barrier [19]. Fig. 8 depicts the building model and the connections between different components. This setup allows for the investigation of the conditions in the BIPV-Back zone. It is worth mentioning that the BIPV-Back zone is part of the interior environment and should not be confused with the ventilation cavity of the BIPV. Additionally, in this work, the BIPV-Back zone is also referred to as the inverter zone, as most placement scenarios for the inverter or power optimiser are implemented in this zone.

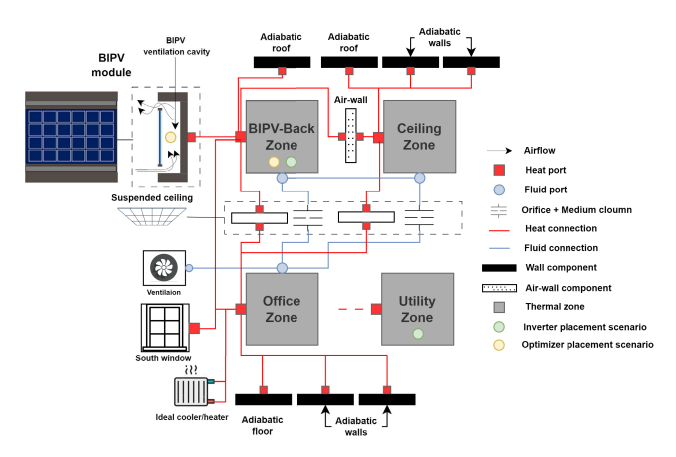


FIGURE 8. Schematic of the building physics model depicts the components and the connections between each of them.

The air exchange between the office and the ceiling zones is calculated using orifice and medium column components to represent the buoyancy effect [20]. The medium column component calculates the airflow based on the stack-effect principle, while the orifice component uses the opening area to calculate the pressure difference between the zones to drive the air exchange. The mass-flow rate is calculated as follows:

$$\dot{m} = C_d \cdot A \cdot \sqrt{2 \cdot \rho_{\text{avg}} \cdot \Delta P_{\text{stack}}} \tag{1}$$

where \dot{m} is the mass flow rate through the column (kg/s), C_d is the discharge coefficient (dimensionless) accounting for flow losses, A is the leakage area of the column (m²), $\rho_{\rm avg}$ is the average air density (kg/m³), typically taken as the average of $\rho_{\rm in}$ and $\rho_{\rm out}$, and $\Delta P_{\rm stack}$ is the pressure difference due to the stack effect (Pa). The discharge coefficient is a parameter for modeling airflow through an opening. It accounts for the effects of friction, turbulence, and contraction as air flows through the opening. The stack pressure is calculated as follows:

$$\Delta P_{\text{stack}} = g \cdot h \cdot (\rho_{\text{out}} - \rho_{\text{in}}) \tag{2}$$

where ΔP_{stack} is the pressure difference due to the stack effect (Pa), g is the acceleration due to gravity (9.81 m/s²), h is the



height of the column (m), ρ_{out} is the density of the air outside the column (kg/m³), and ρ_{in} is the density of the air inside the column (kg/m³).

The office has a south facade with a window that covers 60% of the facade, the frame takes 10% of the window's total area. The BIPV modules cover the facade's top part, which is attached to the ceiling zones. Internal gains from the lighting is modelled to be dissipated in the ceiling zones with a value of 5 W/m² [21]. The office zone setpoint temperature is fixed at 20°C. Regarding the weather conditions, the building simulation used a weather file for Genk, Belgium, obtained from the weather station at EnergyVille. Fig. 9 illustrates the irradiance profile used in the simulations.

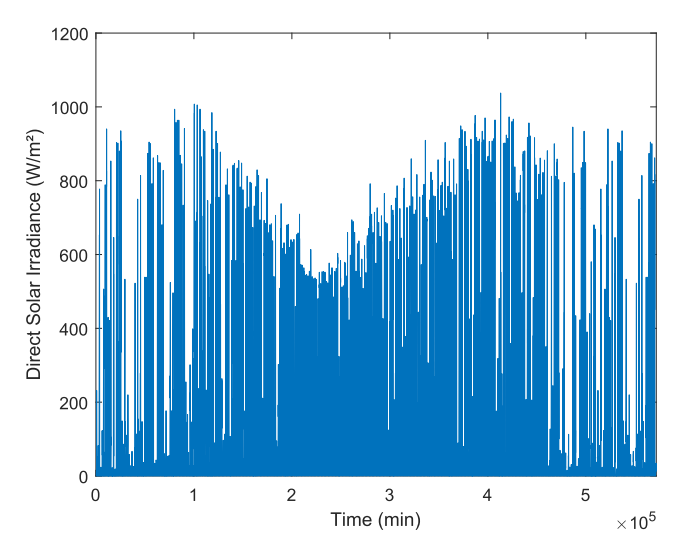


FIGURE 9. Measured irradiance of the south BIPV orientation in Genk (Belgium) used in the simulation.

In addition, a utility room is also modelled to be in a different part of the building, the volume of the utility room is 15.2 m^3 ($2 \text{ m} \times 2 \text{ m} \times 3.8 \text{ m}$). The utility room is a space that is commonly used to house various mechanical, electrical, and plumbing (MEP) systems essential for the building's operation. Hence, the study proposes a scenario to place inverters/power optimisers in the utility room with a controlled temperature set point of 20°C .

E. LIFETIME CONSUMPTION

To evaluate the IGBT lifetime, the CIP08 lifetime model is used [22]. This widely used model is constructed by power cycling different types of IGBTs until failure. This model contains multiple terms that take the cycle and device parameters into account. The key terms in this study are the Coffin-Manson and Arrhenius terms, which represent the effects of minimum cycle temperature and temperature swing on the number of cycles to failure. The model is shown in the equation as follows:

$$N_f = A^{\alpha} \cdot \Delta T_j^{\beta_1} \cdot \exp\left(\frac{\beta_2}{T_{j,min} + 273.15}\right) \cdot t_{on}^{\beta_3} \cdot I^{\beta_4} \cdot V^{\beta_5} \cdot D^{\beta_5}$$
(3)

With N_f the number of cycles to failure, A, β_1 , β_2 , β_3 , β_4 , β_5 constant model parameters, ΔT_j the junction temperature fluctuation, $T_{j,min}$ the cycle minimum temperature, t_{on} the cycle heating time, I the current per bond wire, V the blocking voltage of the chip and D the bond wire diameter. Note that this model is originally fitted on IGBT modules in power cycling testes. The switches used in this study are discrete. There is also an extrapolation of the model, especially in the cycle length. It is therefore important to use the results for a relative comparison instead of absolute lifetime estimations.

To use the CIP08 model, the junction temperature profile needs to be split into load cycles. This is done using a rainflow counting process. Finally, Miner's linear damage rule is used to combine the damage of all individual cycles [23]:

$$\sum_{i=1}^{k} \frac{n_i}{N_i} = C \tag{4}$$

III. SENSITIVITY ANALYSIS

This section presents a sensitivity analysis to assess how key operational parameters influence the lifetime of the DC IGBT. The examined variables include the convection-to-radiation heat loss ratio, the air exchange rate between zones, and the height of the cavity opening. In the analysis, the inverter/optimiser is primarily modeled within the Back-BIPV zone (inverter zone), where different convection-radiation heat loss ratios are evaluated alongside varying air exchange rates. For cases involving cavity placement, a validated BIPV cavity model is employed to investigate the impact of the cavity opening height on the power optimiser's lifetime.

A. RADIATION / CONVECTION RATIO

When the heat is released from the heat sink to the environment, and thus from the thermal RC model to the Modelica model, Modelica requires a ratio of radiative and convective heat flow. The exact ratio of these losses is material and temperature dependent. Because this can greatly increase the complexity of the model, a sensitivity analysis is performed to study how the convection/radiation losses ratio influences IGBT lifetime predictions. Fig. 11 (a) and Fig. 12 (a) show the junction temperature and lifetime estimations for 0%, 25% and 50% radiative losses (and thus 100%, 75% and 50% convective losses). It is clear that there is very little visual difference in the temperature profiles. This is also reflected in the bar plots, with only a difference of 4.6% between the 0% and 50 % cases. It is, therefore, concluded that the ratio of radiative and convective losses is rather limited. It is, therefore, chosen in the remainder of this study to set fixed values for the fraction of convective and radiative energy losses.

B. AIR EXCHANGE

This section investigates the sensitivity of the IGBT lifetime to air exchange between the BIPV-Back zone (inverter/optimiser placement zone) and the ceiling, as well



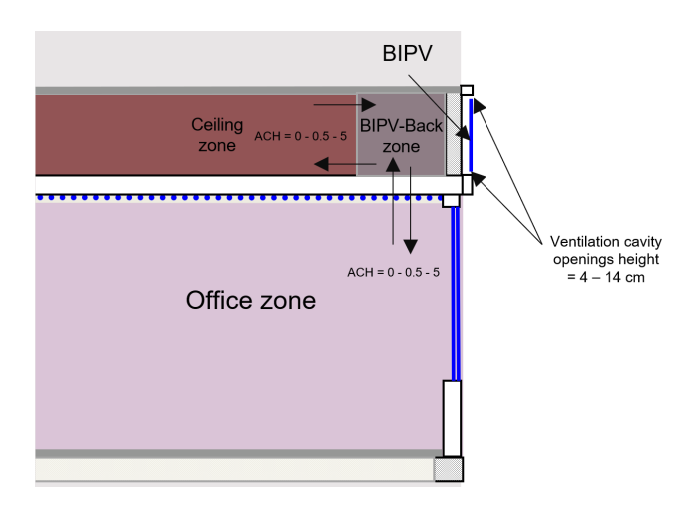


FIGURE 10. Thermal zones of the office space indicating the air exchange parameters (Air change per hour ACH between the zones) to conduct the sensitivity analysis.

as the BIPV-Back zone and the office zone. The air exchange between the BIPV-Back zone and the office depends on the ceiling design. For this sensitivity analysis, three air exchange rates are examined as in Fig. 10. ACH represents the air changes per hour of the zone.

Fig. 11 (b) and Fig. 12 (b) show the IGBT switch temperature and lifetime consumption. Lower air exchange rates cause a positive offset in junction temperature, which is expected since the hot air is trapped inside the BIPV-Back zone. This is also visible in the lifetime consumption plot. A 0.5 ACH and 5 ACH give 7.6% and 14.4% reduction in lifetime consumption compared to the 0 ACH case. An open ceiling with a higher air exchange rate provides a significant increase in lifetime.

The air exchange between the BIPV-Back zone and ceiling is dependent on the design of the building. It can be an open space with sufficient air exchange. However, the airflow can also be blocked by pipes, ventilation tubes, or other systems. This sensitivity analysis examines 2 values for airflow. Fig. 12 (c) shows there is a small increase in temperature when the 5 ACH is compared to the 0.5 ACH case; this results in a 3.8% increase of lifetime consumption as shown in Fig. 11 (c). It can be concluded that airflow between the BIPV-Back zone and the ceiling is less significant, but airflow between the BIPV-Back zone and the office can have a higher impact on the IGBT lifetime.

C. BIPV VENTILATION CAVITY OPENING

This section investigates how the BIPV ventilation cavity opening height can influence IGBT lifetime for the case where the inverter is placed inside the BIPV ventilation cavity. The BIPV module includes two ventilation openings, one at the bottom and one at the top, similar to the configuration shown in Fig. 5. Each opening is 101 cm wide with variable heights ranging from 4 cm to 14 cm. The cavity itself has dimensions of 104 cm width, 11 cm depth, and

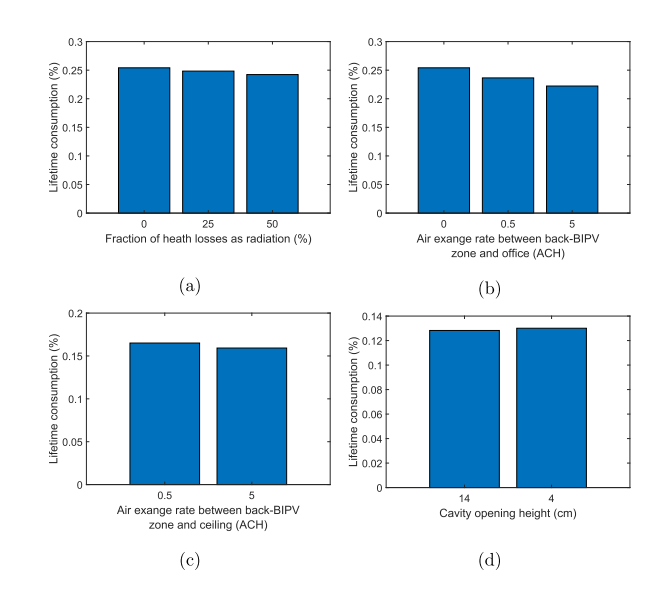


FIGURE 11. Lifetime consumption for multiple (a) fraction of heat loss as radiation, (b) air exchange rate between the Back-BIPV zone and office zone, (c) air exchange rate between the Back-BIPV zone and the ceiling zone, and (d) cavity opening height.

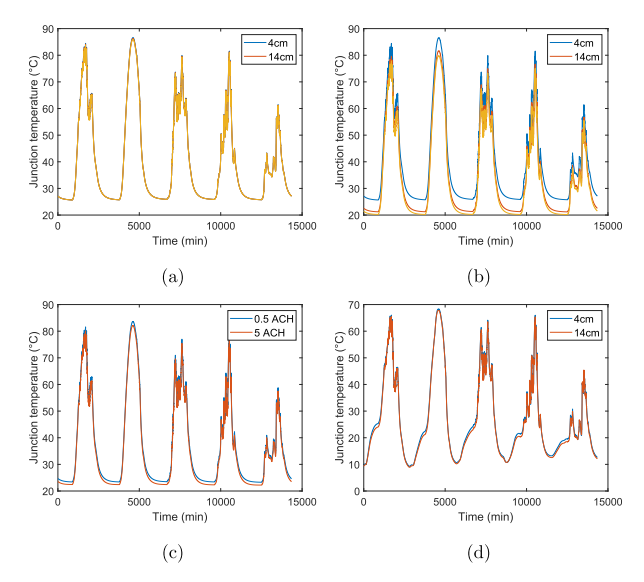


FIGURE 12. Segment of junction temperature for multiple (a) fraction of heat loss as radiation, (b) air exchange rate between the Back-BIPV zone and the office zone, (c) air exchange rate between the Back-BIPV zone and the ceiling zone, and (d) cavity opening height.

99 cm height. Fig. 11 (d) and Fig. 12 (d) show the junction temperature profile and IGBT damage. Increasing the cavity opening height from 4 cm to 14 cm lowers the damage by 1.6%. This is logical because a bigger opening allows for higher airflow, but the effect is very minimal. Also, note that this sensitivity analysis does not take into account the practicality of implementing a full inverter in such a relatively small cavity. It also ignores how the inverter may disturb the airflow.



TABLE 2. Lifetime consumptions in the sensitivity analysis.

0	25	50
0.254	0.248	0.242
0	0.5	5
0.254	0.236	0.222
0	5	
0.165	0.159	
14	4	
	0.254 0 0.254 0 0.165	0.254 0.248 0 0.5 0.254 0.236 0 5 0.165 0.159 14 4

IV. CASE STUDIES

To assess the impact of the different conditions and ventilation strategies on the thermal performance of the power electronic devices in the BIPV systems, various realistic scenarios for inverters and power optimisers were simulated and evaluated. These scenarios consider different placement locations for the devices within the building with varying airflow conditions and environmental control levels to simulate conventional operation environments as in Fig. 8. As in the conducted sensitivity analysis, this analysis focuses on the influence of these factors on component temperatures, cooling effectiveness, and potential implications for longterm reliability. Each case is categorized based on the component type (inverter or power optimiser) to ensure a targeted investigation of their thermal management requirements and performance outcomes. In certain scenarios, the devices are placed above the suspended ceiling; therefore, the type of ceiling plays a crucial role in determining the conditions within the ceiling zone. Primarily, two types are used; isolated and partially open suspended ceilings as in Fig. 13. Ceiling (A) has openings that when combined represent half of the ceiling area. This type is usually used for a better appearance but it also offers higher air exchange between the zones. Ceiling (B) is a common tiles suspended ceiling type that typically is well-isolated which limits the heat transfer and airflow between the zones. These ceilings have U-values of $0.74 \text{ W/m}^2\text{K}$ and $0.6 \text{ W/m}^2\text{K}$ [24]. The discharge coefficient (C_d) varies in each of these cases, primarily influenced by the characteristics of the opening (e.g., sharp-edged, rounded, etc.) [25]. For the case of the half-open ceiling as ceiling A, the discharge coefficient is modelled as 0.65, which is a suitable value that is also used for large openings, louvers and vents [26]. For ceiling B, given that air movement between a room and the ceiling plenum often involves irregular and potentially sharp-edged openings (such as gaps around tiles or fixtures), a discharge coefficient of 0.61 is a reasonable assumption [27]. Regarding the leakage area, Ceiling A has half of the ceiling area open to the plenum space, therefore, the air-leakage area is set to 6 m^2 (total ceiling area is 12 m^2). Ceiling type B leakage area is estimated to be $3 \text{ cm}^2 / \text{ m}^2$ on average for conventional tiles suspended ceiling, therefore, 0.0036 m^2 for the entire ceiling [28].



FIGURE 13. Simulated suspended ceiling types (A) Partially-open ceiling (B) Tiles ceiling.

A. INVERTER PLACEMENT

For this study, 2 inverter locations are considered:

1) ABOVE THE SUSPENDED CEILING

This scenario considers the two types of suspended ceilings as described previously in this section. In the first scenario, the inverter is placed above the suspended ceiling, which is isolated with minimal openings, resulting in limited airflow between the office space and the ceiling zone. This setup restricts natural convection, leading to controlled but less ventilated conditions for the inverter. In the second scenario, the inverter is placed above a partially open suspended ceiling (half of the ceiling is open), allowing for increased airflow between the office space and the ceiling zone. This design promotes enhanced natural ventilation, improving cooling efficiency through convective heat transfer.

2) UTILITY ROOM

The inverter is placed in a utility room with controlled conditions and a temperature set point of 20°C. This scenario provides a benchmark for assessing the effectiveness of controlled environments in minimizing thermal stress and maintaining stable operating temperatures.

Fig. 14 shows the IGBT junction temperature and lifetime consumption for the DC-DC switch and DC-AC switch. Fig. 16 provides a zoom in on February 9th of the junction temperature profile. The best-performing location is the Utility room. The open ceiling and isolated ceiling perform 5,7% and 9,7% worse, respectively, than the utility room for the AC switch, and 6.8% and 10.9% worse, respectively, than the utility room for the DC switch. The difference between the isolated and open ceilings seems to be minimal. Even though there is minimal airflow between the office and the BIPV-back zone in the isolated case, the airflow between the ceiling zone and the BIPV-back zone is sufficient to keep the IGBT temperature within acceptable operating levels. It is also clear that the temperature in the DC switch reaches higher values,



and thus the DC switch experiences more degradation than the AC switch. It can be concluded that placing the inverter in a dedicated utility room can significantly increase the IGBT lifetime.

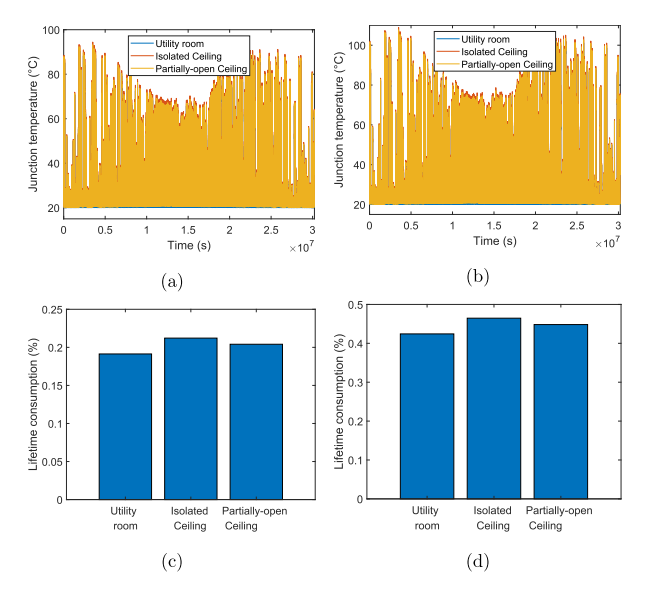


FIGURE 14. (a) Junction temperature and (c) lifetime consumption of the DC switch, and (b) Junction temperature and (d) lifetime consumption of the AC switch for three cases.

B. OPTIMISER PLACEMENT

For this study, 3 optimiser locations are considered:

1) ABOVE THE SUSPENDED CEILING

Similar to the inverter scenario, the power optimiser is placed above the suspended ceiling and evaluated under two ceiling configurations: an isolated ceiling that consists of insulated tiles with restricted airflow and a partially open ceiling that allows higher natural convection. The objective is to analyze whether the increased airflow in the partially open setup provides sufficient cooling for the smaller, heat-sensitive power optimiser compared to the restricted environment of the isolated ceiling.

2) BIPV VENTILATION CAVITY

In this scenario, the power optimiser is installed within the ventilated cavity of the BIPV module. The module follows the same configuration described in Section III-C, with the exception of an opening height of 9 cm. In this setup, the power optimiser is directly exposed to both the external environmental conditions and the thermal effects arising from the BIPV module itself. The analysis focuses on how temperature fluctuations and heat dissipation within the ventilation cavity affect the performance and expected lifetime of the power optimiser.

The year IGBT junction temperature profile and lifetime consumption are shown in Fig. 15. A zoom in on February 9th is provided in Fig. 16. Notice how, in the cavity case, the temperatures drop significantly in winter but are slightly

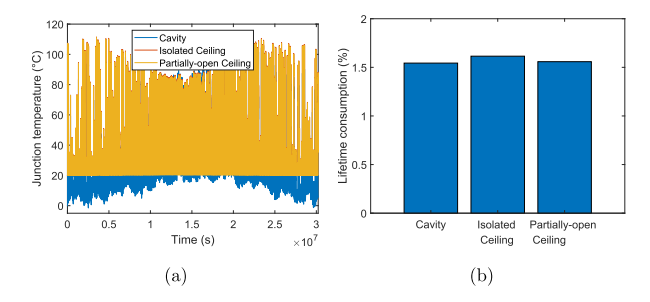


FIGURE 15. (a) Junction temperature and (b) lifetime consumption of the power optimiser DC switch for three cases.

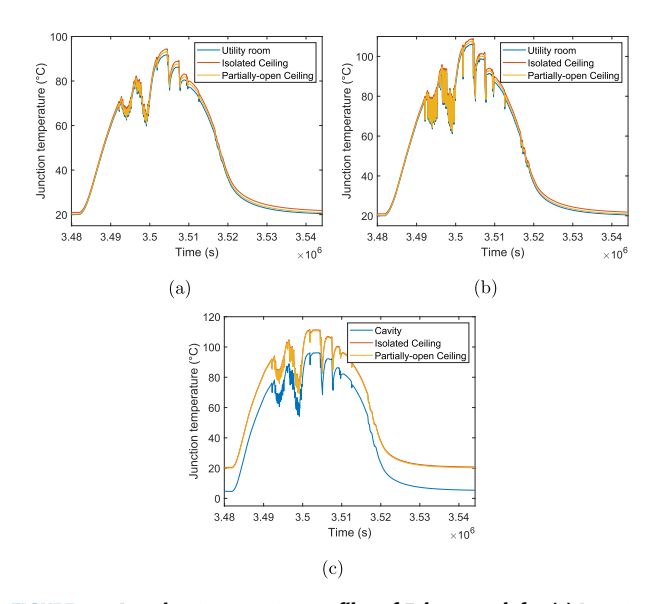


FIGURE 16. Junction temperature profiles of February 9th for (a) Inverter DC switch (b) Inverter AC switch, and (c) Optimiser DC switch.

TABLE 3. Lifetime consumptions for the studied cases.

Inverter location (%)		Utility room	Isolated ceiling	Partially- open ceiling
Lifetime consumption switch inverter (%)	DC	0.191	0.212	0.204
Lifetime consumption switch inverter (%)	AC	0.424	0.465	0.448
Optimiser location		Cavity	Isolated	Partially-
			ceiling	open ceiling

higher in summer compared to other cases. The optimiser in the cavity experiences the least amount of damage. The open and isolated ceiling experiences 1.3 % and 4.5 % increased lifetime consumption than the cavity case. The differences are thus minimal. This might seem nonlogical, but for the cavity case, there are lower minimum temperatures, which are beneficial for a lifetime, but larger temperature swings,



which are worse for lifetime. These effects counteract each other. It can thus be concluded that optimiser placement has minimal effect on IGBT lifetime.

V. CONCLUSION

This study presents a detailed investigation into the thermal and electrical behavior of building-integrated photovoltaic (BIPV) systems, focusing on the performance and lifetime of power optimisers and inverters' switching devices. By integrating power electronics models with building physics frameworks, we assessed the impact of various surrounding factors, such as airflow rates that are achieved in the placement location of the converter on the junction temperature of IGBTs and their long-term reliability. The findings demonstrate that strategic placement and ventilation can play crucial roles in thermal management and system reliability. Optimizing airflow through proper ventilation and reducing the temperature of the placement zone reduces thermal stress and enhances the lifespan of power electronics components. The biggest difference in lifetime consumption simulated in this study was observed in the inverter DC IGBT, where placement in an isolated suspended ceiling results in 10.9 % more lifetime consumption than placement in a utility room. Furthermore, sensitivity analyses indicate that while the choice of airflow rates and BIPV ventilation cavity openings influences the thermal behavior. The placement of inverters in controlled environments, such as utility rooms, remains the most effective strategy for prolonging IGBT lifetimes. This research provides valuable insights into the design and optimization of BIPV systems and their electrical components, offering practical recommendations for enhancing their thermal performance and operational lifespan. Future studies could extend these findings by exploring additional environmental scenarios and further refining the interaction between electrical and thermal models to improve the robustness of BIPV systems in realworld applications. Additionally, future work could address the lifetime of other thermally sensitive components, such as capacitors, the effect of oversizing the components, and how they influence the overall system's reliability.

ACKNOWLEDGMENT

The financial contribution is gratefully acknowledged.

REFERENCES

- [1] I. Kaaya, A. Alzade, S. Bouguerra, N. Kyranaki, A. Bakovasilis, S. Ramesh, D. Saelens, M. Daenen, and A. Morlier, "A physics-based framework for modelling the performance and reliability of BIPV systems," Sol. Energy, vol. 277, Jul. 2024, Art. no. 112730. [Online]. Available: https://www.sciencedirect.com/science/article/pii/S00380 92X24004250
- [2] A. Alzade and D. Saelens, "Assessment of the effects of the cavity in BIPV applications," *J. Phys., Conf. Ser.*, vol. 2654, no. 1, Dec. 2023, Art. no. 012097, doi: 10.1088/1742-6596/2654/1/012097.
- [3] A. Alzade and D. Saelens, "Enhancing BIPV modeling efficiency: A co-simulation framework," in *Proc. Int. Assoc. Building Phys.*, 2025, pp. 575–582.
- [4] I. Kaaya, S. Ramesh, and A. Alzade, "Lifetime prediction of photovoltaic modules: Towards a generalized physics-based approach," in *Proc. 8th World Conf. Photovoltaic Energy Convers.*, 2022, pp. 1–7.

- [5] A. Alzade and D. Saelens, "Developing a framework for automated modelling of BIPV," in *Proc. Building Simul. Conf.*, vol. 18, Sep. 2023, pp. 1117–1124, doi: 10.26868/25222708.2023.1508.
- [6] Y. Peng, S. Zhao, and H. Wang, "A digital twin based estimation method for health indicators of DC–DC converters," *IEEE Trans. Power Electron.*, vol. 36, no. 2, pp. 2105–2118, Feb. 2021, doi: 10.1109/TPEL.2020.3009600.
- [7] A. Abuelnaga, M. Narimani, and A. S. Bahman, "A review on IGBT module failure modes and lifetime testing," *IEEE Access*, vol. 9, pp. 9643–9663, 2021, doi: 10.1109/ACCESS.2021.3049738.
- [8] H. Ye, M. Lin, and C. Basaran, "Failure modes and FEM analysis of power electronic packaging," *Finite Elements Anal. Design*, vol. 38, no. 7, pp. 601–612, May 2002, doi: 10.1016/s0168-874x(01)00094-4.
- [9] F. Jorissen, G. Reynders, R. Baetens, D. Picard, D. Saelens, and L. Helsen, "Implementation and verification of the IDEAS building energy simulation library," *J. Building Perform. Simul.*, vol. 11, no. 6, pp. 669–688, Nov. 2018.
- [10] Y. Amara, R. Boukenoui, R. Bradai, and H. Salhi, "Design and control of two-stage standalone photovoltaic generation system," in *Proc. Int. Conf. Commun. Electr. Eng. (ICCEE)*, Dec. 2018, pp. 1–5, doi: 10.1109/CCEE.2018.8634511.
- [11] L. Van Cappellen, M. Deckers, O. Alavi, M. Daenen, and J. Driesen, "A real-time physics based digital twin for online MOSFET condition monitoring in PV converter applications," in *Proc. 28th Int. Workshop Thermal Investigations ICs Syst. (THERMINIC)*, Sep. 2022, pp. 1–5, doi: 10.1109/THERMINIC57263.2022.9950636.
- [12] F. Liu, Y. Kang, Y. Zhang, and S. Duan, "Comparison of P&O and Hill climbing MPPT methods for grid-connected PV converter," in Proc. 3rd IEEE Conf. Ind. Electron. Appl., Jun. 2008, pp. 804–807, doi: 10.1109/ICIEA.2008.4582626.
- [13] P. D. Reigosa, H. Wang, Y. Yang, and F. Blaabjerg, "Prediction of bond wire fatigue of IGBTs in a PV inverter under long-term operation," in *Proc. IEEE Appl. Power Electron. Conf. Expo. (APEC)*, Mar. 2015, pp. 3052–3059, doi: 10.1109/APEC.2015.7104787.
- [14] P. Fritzson, H. Olsson, and M. Otter, "Modelica—A unified object-oriented language for physical systems modeling, language specification," Modelica Assoc., Linköping, Sweden, Tech. Rep., Sep. 2007.
- [15] C. Martin, A. Urquia, J. Sanchez, S. Dormido, F. Esquembre, J. L. Guzman, and M. Berenguel, "Interactive simulation of object-oriented hybrid models, by combined use of ejs, MATLAB/simulink and modelica/dymola," in *Proc. 18th Eur. Simul. Multiconf.*, 2004, pp. 210–215.
- [16] K. Spiliotis, J. E. Gonçalves, D. Saelens, K. Baert, and J. Driesen, "Electrical system architectures for building-integrated photovoltaics: A comparative analysis using a modelling framework in modelica," *Appl. Energy*, vol. 261, Mar. 2020, Art. no. 114247.
- [17] J. E. Goncalves, T. van Hooff, and D. Saelens, "A physics-based high-resolution BIPV model for building performance simulations," *Sol. Energy*, vol. 204, pp. 585–599, Jul. 2020. [Online]. Available: https://www.sciencedirect.com/science/article/pii/S0038092X20304424
- [18] Y. B. Assoa, L. Mongibello, A. Carr, B. Kubicek, M. Machado, J. Merten, S. Misara, F. Roca, W. Sprenger, M. Wagner, S. Zamini, T. Baenas, and P. Malbranche, "Thermal analysis of a BIPV system by various modelling approaches," *Sol. Energy*, vol. 155, pp. 1289–1299, Oct. 2017. [Online]. Available: https://www.sciencedirect.com/science/ article/pii/S0038092X17306515
- [19] EnergyPlus Engineering Reference: The Reference to EnergyPlus Calculations, National Renewable Energy Laboratory (NREL), Golden, CO, USA, 2023. [Online]. Available: https://energyplus.net/documentation
- [20] M. Wetter, "Multizone airflow model in modelica," in *Proc. 5th Int. Modelica Conf.*, 2006, pp. 431–440.
- [21] B.-L. Ahn, J.-W. Park, S. Yoo, J. Kim, S.-B. Leigh, and C.-Y. Jang, "Savings in cooling energy with a thermal management system for LED lighting in office buildings," *Energies*, vol. 8, no. 7, pp. 6658–6671, Jun. 2015. [Online]. Available: https://www.mdpi.com/1996-1073/8/7/6658
- [22] R. Bayerer, T. Herrmann, T. Licht, J. Lutz, and M. Feller, "Model for power cycling lifetime of IGBT modules—Various factors influencing lifetime," in *Proc. 5th Int. Conf. Integr. Power Electron. Syst.*, Mar. 2008, pp. 1–6.
- [23] M. A. Miner, "Cumulative damage in fatigue," J. Appl. Mech., vol. 12, no. 3, pp. A159–A164, Sep. 1945, doi: 10.1115/1.4009458.
- [24] C. Jimenez-Bescos, "The effect of suspended ceilings on thermal mass to reduce overheating," Dept. Eng. Built Environ., Publications Office Eur. Union, Anglia Ruskin Univ., CM, U.K., Tech. Rep., 2015, pp. 821–826.



- [25] M. Haghbin and A. Sharafati, "A review of studies on estimating the discharge coefficient of flow control structures based on the soft computing models," Flow Meas. Instrum., vol. 83, Mar. 2022, Art. no. 102119. [Online]. Available: https://www.sciencedirect.com/science/article/pii/ S0955598621002156
- [26] C. Zhang, Q. Chen, P. Heiselberg, and M. Pomianowski, "Airflow pattern and performance analysis of diffuse ceiling ventilation in an office room using CFD study," in *Proc. Building Simul. Conf.*, Dec. 2015, pp. 925–932.
- [27] P. Karava, T. Stathopoulos, and A. K. Athienitis, "Wind driven flow through openings—A review of discharge coefficients," *Int. J. Ventilation*, vol. 3, no. 3, pp. 255–266, Dec. 2004, doi: 10.1080/14733315.2004.11683920.
- [28] C. Younes, C. A. Shdid, and G. Bitsuamlak, "Air infiltration through building envelopes: A review," *J. Building Phys.*, vol. 35, no. 3, pp. 267–302, Jan. 2012, doi: 10.1177/1744259111423085.



LEANDER VAN CAPPELLEN received the M.S. degree in electronics and ICT engineering, in 2020. He is currently pursuing the Ph.D. degree in energy systems engineering with Hasselt University, Hasselt, Belgium. Since 2020, he has been a Researcher with the Energy Systems Engineering (ESE) Group, imo-imomec. His current research interests include, but are not limited to, power electronics reliability, condition monitoring, and renewable energies.



ABDELLA ALZADE received the B.Sc. degree in mechanical engineering from Eastern Mediterranean University, Cyprus, and the M.Sc. degree in renewable energy engineering and management from the University of Freiburg, Germany. He is currently pursuing the Ph.D. degree in civil engineering with KU Leuven, Belgium. His work emphasizes optimizing renewable energy integration in building systems to enhance energy efficiency and sustainability. He has contributed

to multiple conferences and journals in the field of energy systems for buildings and has participated in projects aimed at advancing BIPV technology applications. His research focuses on building energy systems, with expertise in modeling and simulating building-integrated photovoltaic (BIPV) systems.



DIRK SAELENS received the M.Sc. degree in architectural engineering and the Ph.D. degree in civil engineering from KU Leuven, Belgium, in 1997 and 2002, respectively. His doctoral research focused on ventilated double-skin facades within the Building Physics Section. In 2005, he joined VK Engineering, Belgium, as a Project Engineer, where he specialized in designing energy-efficient and comfortable buildings, including NATO HQ and a new hospital in Mechelen. Currently, he is

a Full Professor in energy in buildings and the Head of the Building Physics and Sustainable Design Section, Department of Civil Engineering, KU Leuven. At EnergyVille, he co-coordinates the Buildings and Districts Research Line and a member of the Operational Steering Committee. In 2002, he received a postdoctoral fellowship from Flemish Agency for Innovation by Science and Technology (IWT). His expertise is in energy and comfort assessment in buildings and urban environments, supported by simulations and field measurements. He has approximately 350 publications, including peer-reviewed articles, books, and conference proceedings; and has an H-index of 28 (WoS) and 39 (Google Scholar).



MICHAËL DAENEN received the M.S. degree in applied physics from Eindhoven University of Technology (TU/e), Eindhoven, The Netherlands, in 2004, and the Ph.D. degree in material physics, on the topic of nano crystalline diamond synthesis and characterization from Hasselt University, Hasselt, Belgium, in 2008. Since 2014, he has been a Professor of engineering technology with Hasselt University. His research is spread over the Wafer PV and Module Team and the Energy System

Team, Imo-Imomec. He focuses on the reliability of PV modules and PV systems and integrated PV, such as BIPV, IIPV, and Agri PV. He is the author of three U.S. patents and more than 80 articles published in high-quality journals and conferences. He is a reviewer of high-quality international journals and conferences.

• • •